

# Evolution of Ice Wedge Junction Angles in an Arctic Point Bar

Rowan Biessel

## Abstract

Ice wedges, which form as water fills thermal contraction cracks and refreezes, underlay much of the Arctic and form stark networks of patterned ground that can be seen aerially. To answer questions related to the role ground ice plays in the Arctic's landscape evolution, I assess the utility of using ice wedge junction angles as a proxy for the surface's relative age. I test this technique by quantifying junction angle evolution in progressively older point bar deposits along Alaska's Coville River. In the studied point bar, the youngest junctions tend to have the most 90 and 180° angles and the least 120° angles. However, each surface, except for the youngest, had statistically similar junction angle distributions. This implies that if an age relation does exist, it likely saturates quickly. This limits the utility of such an analysis for studying surface chronologies of surfaces that are more than several hundred years old, like such as like drained thermokarst lake basins.

## 1 Introduction

In the Arctic, polygonal ground is a ubiquitous expression of ice-rich permafrost, a principal control on the Arctic's geomorphology (Zwieback et al., 2023; Jones, Grosse, Arp, et al., 2015), ecology (Walker et al., 1994; M. T. Jorgenson et al., 2022), water resources (Fedorov et al., 2014), energy budget (van Huissteden, 2020). Ice wedges, massive aggregates of ice that form in thermal contraction cracks, are responsible for the patterned/polygonal ground appearance that can be seen from remote sensing imagery.

Under Pleistocene and Holocene climactic variations, as well as landcover disturbances, ice wedges have undergone various stages of degradation and stabilization (Kanevskiy et al., 2017). Thermokarst lakes (an example is shown in Fig. 1), as well as drained lake basins, dot Arctic landmasses, which represent the final stages of ice-wedge/permafrost degradation while also providing lacustrine deposits for the formation of new permafrost and aggra-

dation of new ice wedges (Jones, Grosse, Farquharson, et al., 2022). The dynamics of these systems are still being understood – particularly whether they are a cyclic process or the current mosaic is representative of a more linear chronology starting at the beginning of the Holocene (M. Torre Jorgenson et al., 2007).

Extensive remotely sensed chronologies, beyond sparse coring/carbon dating, of ice-wedge aggradation could more thoroughly evaluate these hypotheses to reconstruct the spatiotemporal dynamics of ice-wedge aggradation in drained lake basins and adjacent geomorphic units. In turn, understanding the chronology of ice-wedge aggradation/cycling will be important for predicting how ice-rich permafrost responds to current warming trends and how this will broadly impact Arctic landscapes.

Here, I quantify ice-wedge junction angles in meandering point bars to evaluate the relevance of polygonal ground morphometry to surface relative aging. Like drained lake basins, point bars are thermally and mechanically reworked surfaces that allow for the initiation of new ice wedges. The chronologies of point bar sequences are better understood, providing a convenient way to assess remotely sensed-based dating methods.

### 1.1 Formation and Morphometry of Polygonal Ground

Polygonal ground is related to thermal contraction cracking in polar regions, desiccation cracking in drained basins, or jointing in cooling lavas. Both cooling and desiccation generate tensile stresses in the respective media, which lead to the nucleation of cracks at, often randomly, distributed weak zones (Goehring, 2013; Black, 1982). As a crack propagates towards another, it curves into those nearby cracks, forming 90-degree angles—T-

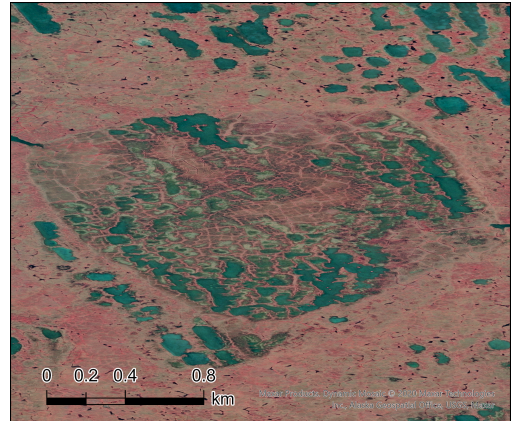


**Figure 1.** An example of a thermokarst drained lake basin with polygonal ground in Alaska’s Arctic Coastal Plain.

junctions. Numerous form polygonal networks at varying scales depending on the tensile strength of the material, its thickness, (Goehring, 2013), and the temperature/moisture gradient. In wet Arctic environments, snow or liquid water infiltration during the summer leads to meter-wide ice-wedge growth over  $10^3$  years timescales. (Black, 1982; Lachenbruch, 1962).

Prior cracks act as weak zones, leading to repeated fracture cycles along the same general paths. Experiments and observations in desiccation environments show that the crack junction locations migrate, and angles between cracks evolve from T-junctions to more regular 120-120-120 degree Y-junctions (Goehring, 2013). While the predominant shape of polygons, rectangular shapes are sometimes attributed to gravitational influences on the stress field on sloping surfaces (Zhang et al., 2022) or the constraining shape of the sedimentary deposits (Sylvester, 2023). However, the first-order shape of the polygon is likely independent of the junction angles, as rectangular polygons may still locally intersect at Y-junctions.

The principal objective of this study is to establish a relationship, or lack thereof, between junction angle distribution and relative age. The extent to which junction evolution occurs in ice wedges is uncertain, and remote sensing studies of polygon junction angles in the Arctic have not yet been performed. While Sylvester (2023) has hypothesized that the shape of ice-wedge polygons in Siberian point bars is related to the stability of meander rates, this hypothesis is based on the first-order polygon shape and not the local geometry of the junctions themselves.

## 2 Data, Study Area, and Methods

Alaska's Colville River flows Northeast from the foothills of the Brooks Range through the Arctic Coastal Plain and empties into the Arctic Ocean. The entire length of the river lies above continuous permafrost. Its delta has abundant polygonized point bars, making it an ideal location to study the recent evolution of ice-wedge polygon junctions.

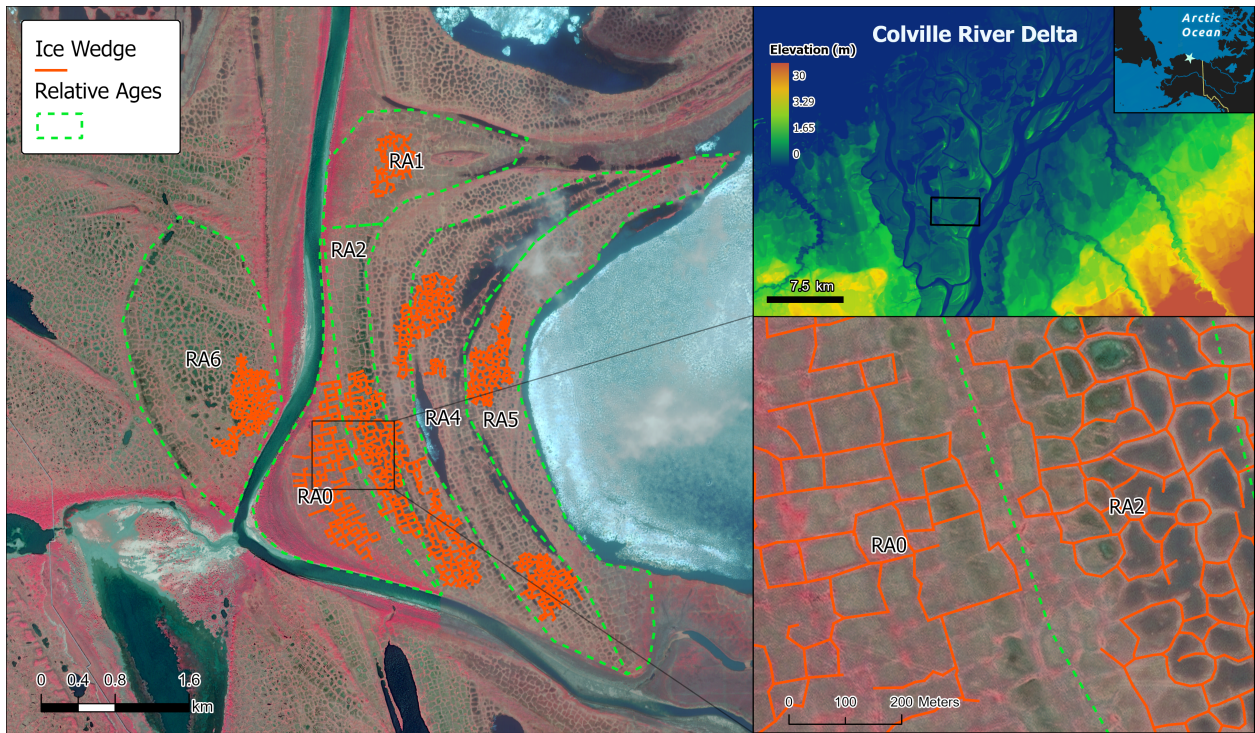


**Figure 2.** A map showing one of the proposed point bar study sites with Maxar CIR base imagery. The first inset shows the DSM of the region from 2022.

Using a 50cm resolution Color Infrared (CIR) base map of Alaska (Maxar Worldview-2 and Geospatial-2), I mapped ice-wedges (yielding 2607 junctions) across six units of different relative ages (RA) along a point bar in the Colville River Delta. This imagery is a composite of Geoeye-1 (acquired 2020-06-24), Worldview-2 (2016-07-14), and Worldview-3 (2018-10-03). I also used the 2m ArcticDEM digital surface model (DSM) from 2022 as a supplemental dataset. Examples of these data and the study area are shown in Fig. 2.

I mapped the polygon edges in ArcGIS Pro (see Fig. 2), capturing any curvature of the ice wedge. In the CIR imagery, these features are highlighted by either dark water-filled troughs or raised vegetated rims/edges that stand out in the near-infrared. In order to ensure the lines intersect without creating spurious extra junction angles, I used snapping and the split tool, followed by the “Remove Small Lines” tool to eliminate any excess lines. Combining these procedures ensures the resulting polyline network perfectly

intersects without spurious edges. To maintain a high-quality junction dataset, I excluded ice wedges or junctions poorly defined in the available imagery.

To quantify junction angles, I iterated over each unique pair of features to establish sets of intersecting lines. The initial ordering of each line is arbitrary, so I first measured each angle with respect to north, wrapping only between 0 and 360 degrees. Each line also may contain multiple vertices, and the junction angles must be computed relative to the point on that line nearest to the junction. To select the correct line segment, I minimized the distance of each point in the line to the junction. From each angle relative to north ( $0^\circ$ ), the angles can be sorted and differenced to recover the adjacent junction angles. This algorithm consistently yields sets of angles that sum to 360 degrees.

I estimated the junctions' relative surface ages (RAs) based on point bar and scroll bar progression from the current river channel. I recorded the RAs as integers, with the youngest surface 0 (RA0). I also studied a population of ice-wedge polygons on the opposite side of the river meander, which I interpret as the oldest (RA6). I also split what was originally just RA1 into RA2 and RA1 due to the apparent preliminary differences in polygon morphometry and to account for upstream translation in the river migration. These units are shown in Fig. 2.

I compared the estimated junction angles in the different relative age units using a two-sided Kolmogorov-Smirnov (KS) test (using `scipy`). I also computed kernel density estimates of the empirical probability density functions (PDFs). I then estimated the least squares linear fit versus RA for bins of  $\pm 5^\circ$  around  $180^\circ$ ,  $90^\circ$ , and  $120^\circ$ . While there isn't a strong expectation that any relationship should be linear, this provides some sense as to whether these angle bins are becoming relatively more or less abundant.

### 3 Results

The kernel density estimates of the quantified junction angles for each RA are shown in Fig. 3. Each unit shows a relatively high proportion of junction angles around  $180^\circ$  while the youngest unit has the most  $90^\circ$  junctions and the least  $120^\circ$  angles. Generally, this



**Figure 3.** Kernel density estimates of the probability density function for the measured junction angles at each relative age. Full black horizontal lines denote where angles are expected to concentrate for T-junctions, while angles are expected to concentrate 120 degrees for Y-junctions (dashed horizontal line.)

corresponds to an increase in Y-junctions in the older units. The youngest also shows the most independence from the other populations (see Fig. 4). However, the older units (RA1–RA6) don't appear to be independent of each other, with KS test p-values typically between 1 and 0.1.

Although R2 appeared different from R1 while mapping these units, the KS-test p-value is still large compared to every population except R0, suggesting it isn't. Despite this result, the R1 population of angles striking has very few 120° angles. This feature is missing from every other older population, with comparable numbers of 120° angles as 90° angles. In addition, R1 also has the fewest 180° angles.

Inspecting the evolution of just the 90°, 120°, and 180° junction angles, shown in Fig. 5, the biggest differences are again between the RA0 unit and the others. Such differences create a weak trend with age in each case. Linear trend estimates are  $-0.67 \pm 0.044 RA^{-1}$ ,

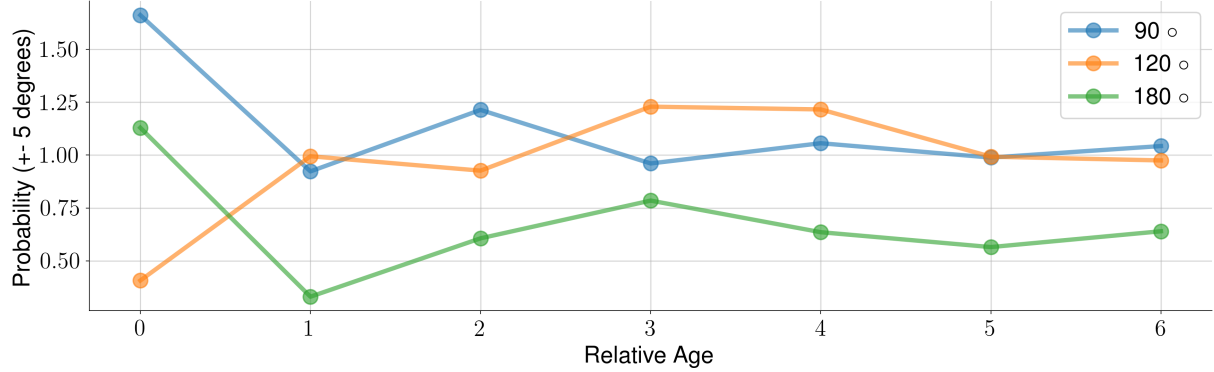


**Figure 5.** Probability density for the angles of interest by RA, summed over  $\pm 5^\circ$  bins.

$0.71 \pm 0.48 RA^{-1}$ , and  $-0.035 \pm 0.048 RA^{-1}$  for the  $90^\circ$ ,  $120^\circ$  and  $180^\circ$  bins respectively.

Any such non-zero trends appear to be driven by the difference between RA0 and the other units. From R1 and older, there appears to be little variation between the proportions of these angles. However, these trends are consistent with the hypothesis that the older units will have an increasing proportion of Y-junctions.

#### 4 Discussion

Disparate timescales between meander-depositional rates and ice-wedge maturation may explain the lack of independence between the older (RA 1-6) junction angles. Erosion rates range from 1-3m/yr for parts of the Colville River near Niqusit, AK (Payne et al., 2018). Assuming equivalent and constant deposition, this would put the RA2 unit at roughly 500-1500 years old. Depending on the climactic history of this site, these ice wedges may have experienced up to 1500 thermal fracture cycles, possibly exceeding a Y-junction saturation equilibrium

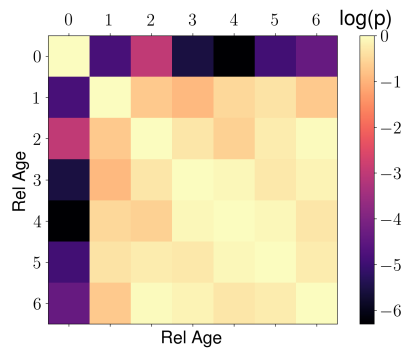


**Figure 4.** KS test  $\log_{10} p$ -values for each pair of junction angle distributions.

time. For comparison, desiccation cracks tend to saturate at  $120^\circ$  by the 10th cycle (Goehring, 2013).

A  $10^2$  year saturation timescale puts limitations on the utility of junction-angle studies for reconstruction chronologies that extend to the beginning of the Holocene, which is the case for drained lake basin systems that have been radiocarbon dated (M. Torre Jorgenson et al., 2007). While full chronologies may not be able to be recovered, the relative comparison of Y-junctions and T-junctions with the presented methodology may be able to, in a binary way, separate new ice wedges from early Holocene ones. For instance, populations of ice wedges with highly orthogonal junctions may point towards more recent secondary lake drainage events within older drained lake basins.

The difference between RA0 and RA1 may also be due to a combination of uncertainty in junction angle estimation and factors such as the basin geometry. For instance, the generally rectangular shape of the polygons may bias mapping of the junction angles towards  $90^\circ$  or  $180^\circ$  despite the actual angles being less orthogonal. The resolution of the imagery and the wideness of the ice wedges may also obscure localized Y-junctions, making them appear as T-junctions. Studies of additional point bar systems, with additional analysis of the point bar's morphometry, may help to ascertain whether such constraining geometry is an important factor.

## 5 Conclusions

Ice wedges are ubiquitous features of Arctic landscapes and are also present on Mars. Understanding what the age controls on ice-wedge junction morphology will allow for better constraints into processes that have reworked the Arctic landscape in the Pleistocene and Holocene. Here, I've used a combination of manual mapping and morphometric analysis in Python to quantify junction angles between intersecting ice wedges with respect to progressively older point bar deposits. While I found that the age relationship with ice-wedge junction saturates relatively quickly, in several hundred years, there is a promise

for junction angle analyses to aid our understanding of relatively recent periods of ice-wedge aggradation and permafrost development.

## 6 Open Research

The code used to perform these analyses, along with shapefiles of the mapped ice wedges and relative age units, can be found in the following GitHub repository:  
<https://github.com/rbiessel/IceWedgeJunctionAngles>.

## 7 Acknowledgements

I want to thank Michael Mellon for a constructive discussion on patterned ground and potential project ideas.

## References

- Black, Robert F. (1982). “Ice-Wedge Polygons of Northern Alaska”. In: *Glacial Geomorphology*. Ed. by Donald R. Coates. Dordrecht: Springer Netherlands, pp. 247–275. ISBN: 978-94-011-6491-7. DOI: 10.1007/978-94-011-6491-7\_9.
- Fedorov, A. N. et al. (2014). “Estimating the Water Balance of a Thermokarst Lake in the Middle of the Lena River Basin, Eastern Siberia”. In: *Ecohydrology* 7.2, pp. 188–196. ISSN: 1936-0592. DOI: 10.1002/eco.1378.
- Goehring, Lucas (Dec. 13, 2013). “Evolving Fracture Patterns: Columnar Joints, Mud Cracks and Polygonal Terrain”. In: *Philosophical Transactions of the Royal Society A: Mathematical, Physical and Engineering Sciences* 371.2004, p. 20120353. DOI: 10.1098/rsta.2012.0353.
- Jones, Benjamin M., Guido Grosse, Christopher D. Arp, et al. (Oct. 29, 2015). “Recent Arctic Tundra Fire Initiates Widespread Thermokarst Development”. In: *Scientific Reports* 5.1 (1), p. 15865. ISSN: 2045-2322. DOI: 10.1038/srep15865.
- Jones, Benjamin M., Guido Grosse, Louise M. Farquharson, et al. (Jan. 2022). “Lake and Drained Lake Basin Systems in Lowland Permafrost Regions”. In: *Nature Reviews Earth & Environment* 3.1, pp. 85–98. ISSN: 2662-138X. DOI: 10.1038/s43017-021-00238-9.
- Jorgenson, M. T. et al. (Sept. 1, 2022). “Rapid Transformation of Tundra Ecosystems from Ice-Wedge Degradation”. In: *Global and Planetary Change* 216, p. 103921. ISSN: 0921-8181. DOI: 10.1016/j.gloplacha.2022.103921.

- Jorgenson, M. Torre and Yuri Shur (2007). "Evolution of Lakes and Basins in Northern Alaska and Discussion of the Thaw Lake Cycle". In: *Journal of Geophysical Research: Earth Surface* 112.F2. ISSN: 2156-2202. DOI: 10.1029/2006JF000531.
- Kanevskiy, Mikhail et al. (Nov. 2017). "Degradation and Stabilization of Ice Wedges: Implications for Assessing Risk of Thermokarst in Northern Alaska". In: *Geomorphology* 297, pp. 20–42. ISSN: 0169555X. DOI: 10.1016/j.geomorph.2017.09.001.
- Lachenbruch, Arthur H. (Jan. 1, 1962). "Mechanics of Thermal Contraction Cracks and Ice-Wedge Polygons in Permafrost". In: *Mechanics of Thermal Contraction Cracks and Ice-Wedge Polygons in Permafrost*. Ed. by Arthur H. Lachenbruch. Vol. 70. Geological Society of America, p. 0. ISBN: 978-0-8137-2070-8. DOI: 10.1130/SPE70-p1.
- Payne, Cole, Santosh Panda, and Anupma Prakash (Mar. 2018). "Remote Sensing of River Erosion on the Colville River, North Slope Alaska". In: *Remote Sensing* 10.3 (3), p. 397. ISSN: 2072-4292. DOI: 10.3390/rs10030397.
- Sylvester, Zoltan (Nov. 9, 2023). "A Frozen History of Meandering: Mapping and Modeling Permafrost Polygons on Point Bars". Webinar. Permafrost Discovery Gateway Webinar Series.
- Van Huissteden, J. (2020). "The Energy Balance of Permafrost Soils and Ecosystems". In: *Thawing Permafrost*, pp. 51–106. DOI: 10.1007/978-3-030-31379-1\_2.
- Walker, Marilyn D., Donald A. Walker, and Nancy A. Auerbach (1994). "Plant Communities of a Tussock Tundra Landscape in the Brooks Range Foothills, Alaska". In: *Journal of Vegetation Science* 5.6, pp. 843–866. ISSN: 1654-1103. DOI: 10.2307/3236198.
- Zhang, Lei, Yang Lu, and Jinhai Zhang (Jan. 2022). "A Polygonal Terrain on Southern Martian Polar Cap: Implications for Its Formation Mechanism". In: *Remote Sensing* 14.22 (22), p. 5789. ISSN: 2072-4292. DOI: 10.3390/rs14225789.
- Zwieback, Simon et al. (2023). "Disparate Permafrost Terrain Changes after a Large Flood Observed from Space". In: *Permafrost and Periglacial Processes* 34.4, pp. 451–466. ISSN: 1099-1530. DOI: 10.1002/ppp.2208.